Controlling the Passage of Light through Metal Microchannels by Nanocoatings of Phospholipids

Shannon M. Teeters-Kennedy,[†] Kenneth R. Rodriguez,[†] Trisha M. Rogers,[†] Keith A. Zomchek,[†] Shaun M. Williams,[†] Alexandra Sudnitsyn,[†] Lauren Carter,[†] Vadim Cherezov,[†] Martin Caffrey,[‡] and James V. Coe*[,†]

Department of Chemistry, The Ohio State University, Columbus, Ohio 43210-1173, and Department of Chemical and Environmental Sciences and Materials and Surface Science Institute, University of Limerick, Limerick, Ireland

Received: April 9, 2006; In Final Form: August 24, 2006

The flow of polarized light through a metal film with an array of microchannels is controlled by the phase of an optically active, phospholipid nanocoating, even though the coating does not cover the open area of the microchannels. The molecular details of the assembly (DPPC phospholipid monolayer/bilayer on a hexadecanethiol monolayer on a copper- or nickel-coated microarray) were determined using the infrared, surface-plasmon-mediated, extraordinary transmission of the metal microarrays. Infrared absorption spectra with greatly enhanced absorptions by comparison to literature were recorded and used as a diagnostic for the phase, composition, and molecular geometry of these nanocoatings. This approach presents new tools for nanoscale construction in constricted microspaces, which may ultimately be useful with individual microchannels.

Introduction

Metallic microarrays of holes combine unusual optical properties with the ability to serve as scaffolding for the construction of nanoscale assemblies within the channels. The gridded arrangement can facilitate integration with microarrayed detectors and the macroscopic world. The small molecular quantities required to coat individual microchannels are attractive regarding arrayed detection methods and combinatorial techniques often used in analytical chemistry and biochemistry. Likewise, control of the passage of light through microchannels may be useful for sensing or manipulating the contents of individual microchannels. The potential of Ebbesen's extraordinary transmission effect[1] for optical switching with metal nanoarrays has been demonstrated with liquid crystal films[2,3] and polymer films doped with photochromic molecules.[4] In this work, we use the extraordinary transmission to characterize the nanocoatings, but the optical switching is not based on the extraordinary transmission effect (which occurs in the infrared region with our meshes). The present application of a thermooptical switch is interesting because only a monolayer of optically active medium is required and the monolayer does not cover the openings of the microchannels. Thermooptical switches have been described in the literature with potential applications in molecular devices[5] and phased-array antennas.[6]

The thermooptical switch in this work is based on a change in the optical polarization properties of two different phases of the natural phospholipid molecule dipalmitoylphosphatidylcholine (L-DPPC). This phospholipid is a major component in lung surfactant[7] and is about 5% of the lipid content in red blood cell membranes.[8] In order for a phospholipid nanocoating to control the passage of light through a microchannel, the light must pass along the surface of the channel rather than through the volume of the hole. This is achieved by only selecting linearly polarized light that has been rotated by the microchannel's metal surface. An image of a single 6 μm square microchannel using a polarized optical microscope in transmission mode with the polarizers aligned (0°) is shown on the left side of Figure 1. The light flows through the volume of the hole. Upon rotating one of the polarizers by 90°, the microscope user no longer sees any light coming from the sample. However, the image on the right side of Figure 1 results if the attached camera is set to image for a period 100 times longer. This image suggests that the rotated light flows along the surface of the metal microchannel. This light flows through any surface molecules and can potentially be controlled by surface coatings.

The surface coating in this work consists of the optically active phospholipid molecule 1,2-dipalmitoyl-*sn*-glycero-3-phosphocholine (L-DPPC). A space-filling model of DPPC is shown on the left of Figure 2 with the glycerol unit indicated with a dashed oval. The second or middle carbon atom of the glycerol unit bonds to four different chemical moieties and is therefore chiral. The zwitterionic headgroup with hydrophobic chains favors layered assemblies. In our trilayer system (see Figure 2, middle), the phospholipid bilayer is built upon a hydrophobic layer, resulting in a bilayer orientation reversed from that of cell membranes. Removal of the top layer then results in a hybrid bilayer system with adsorbed water helping to stabilize the DPPC monolayer (see Figure 2, right).

Nature uses mixtures of phospholipids in cell membranes to adjust phase and flexibility for specific functions.[8] Temperature, polar headgroup, chain length, and saturation in the chains all affect membrane fluidity. At room temperature, fully hydrated DPPC molecules assume a lamellar gel phase ($L_{\beta'}$) where the tails are in an all-trans configuration with a slight tilt (perhaps 14° relative to the membrane normal[9]). At higher temperatures, the lipid changes to a lamellar liquid crystalline phase (L_α) in which its tails are more fluid, there is diffusion in the lateral plane of the bilayer, and there are increased numbers of gauche

* Corresponding author. E-mail: coe.1@osu.edu.
[†] The Ohio State University.
[‡] University of Limerick.

10.1021/jp062201g CCC: $33.50
Published on Web 09/30/2006

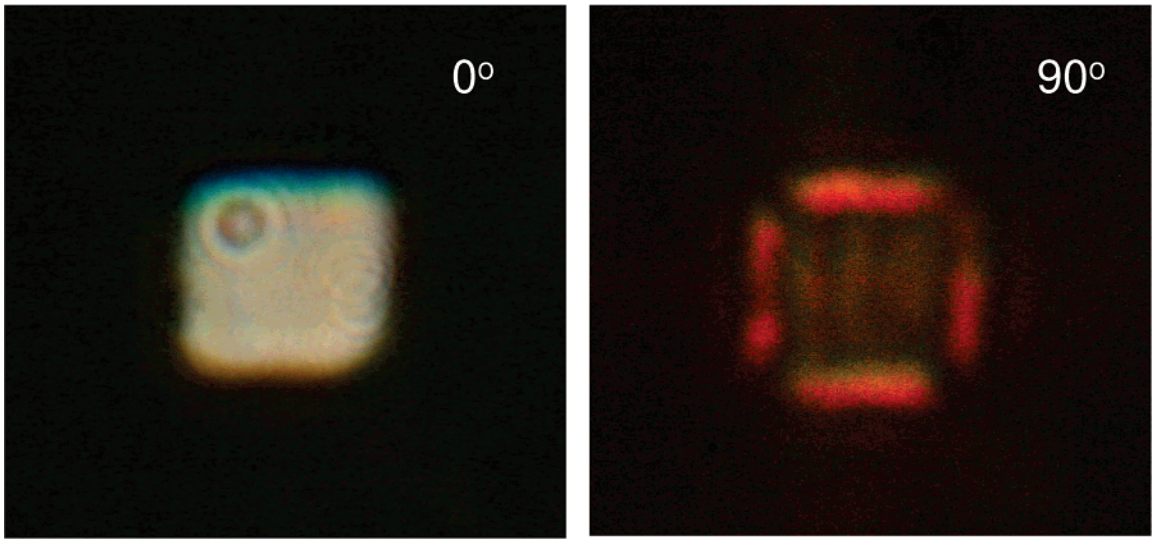

Figure 1. Polarized optical microscope images (100× objective, 20× eyepiece, and 10 cm extended camera position) of a single 6 μm square microchannel in nickel with polarizers aligned (0°, left) and polarizers opposed (90°, right, with a 100-fold longer intergration time). Aligned polarizers (left) allow light to travel through the volume of the hole, while polarizers at 90° select against the volume transmission and select for light rotated by its interaction with the metal surface.

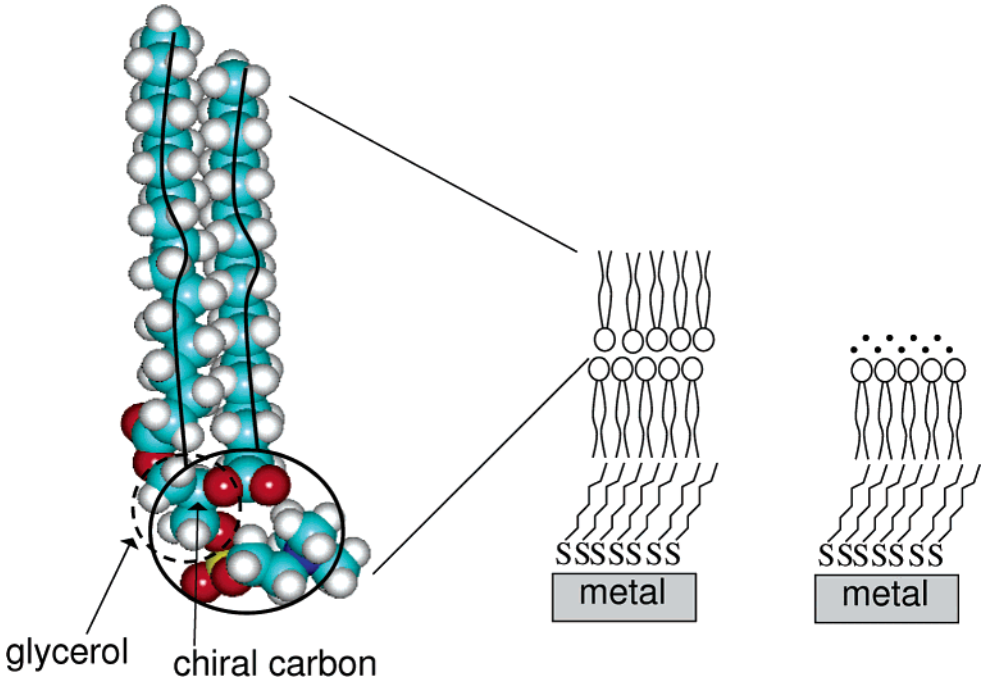

Figure 2. Schematic of trilayer and bilayer systems. A mesh with an array of subwavelength holes is coated with a self-assembled monolayer of 1-hexadecanethiol (zigzag lines attached to metal through S-atoms) and then a bilayer of optically active dipalmitoylphosphatidylcholine (L-DPPC) (see middle drawing). The DPPC molecule consists of a hydrophilic polar headgroup (indicated with a circle) and two hydrophobic, 16-carbon-long, hydrocarbon fat chains (indicated with curvy lines). Optical activity associated with a chiral center arises from the middle carbon in the glycerol subunit. Hydrating the mesh with phospholipid bilayer allows the removal of the top layer of lipid (right drawing where the dots represent water molecules).

(bent) configurations in the hydrocarbon chains. The transition to the L_α phase is very important in nature because phospholipids in cell membranes must usually be in a fluid state for membrane-embedded proteins to function. This transition, hereafter referred to as the chain melting transition, occurs at ~41 °C for fully hydrated DPPC in vesicles[10] and in multilayers.[11] A completely anhydrous DPPC bilayer undergoes the transition at 80 °C.[12] The underlying hexadecanethiolate monolayer in the sample used in this study is also in a crystalline gel phase, but its chain melting transition occurs above 100 °C and therefore the thiolate is not expected to melt in the temperature range of the phospholipid transition. The trans hydrocarbon chains generally tilt relative to the surface normal (tilt angles from 15 to 30° have been reported[13−15]). Changes in the phase of phospholipid/water systems have been routinely tracked by polarized optical light microscopy, as well as other properties such as birefringence, refractive index, turbidity, and scattered light.[16−19]

In this work, the extraordinary infrared transmission of copper-coated, nickel meshes (or bare nickel meshes) with arrays of subwavelength apertures is used to characterize the phase and composition of self-assembled nanocoatings. These meshes have sufficiently large infrared (IR) transmissions that they can be placed in the sample position of routine Fourier transform

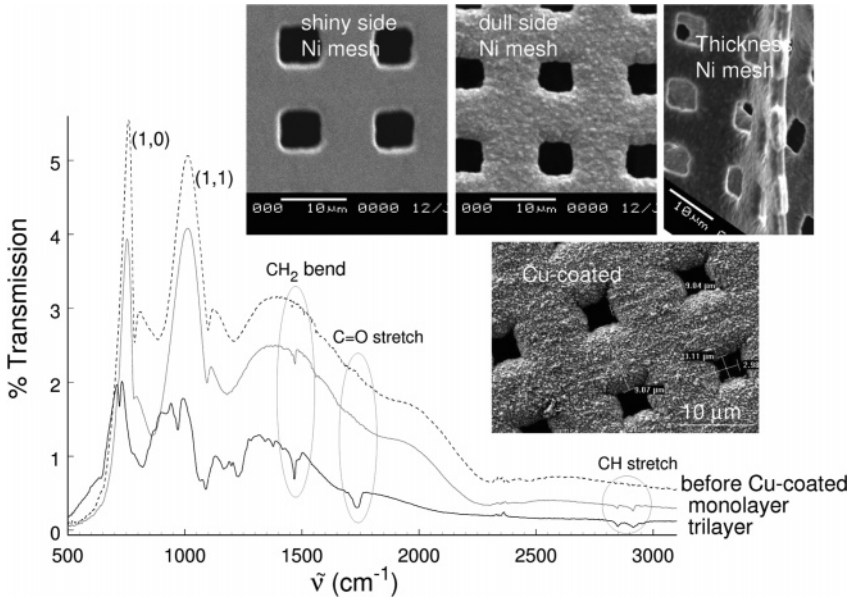

Figure 3. IR transmission spectra at 4 cm^{-1} resolution of copper-coated mesh before (top dashed trace) and after coating with 1-hexadecanethiol (middle gray trace) and DPPC (bottom solid trace). The three images near the top are SEMs of the smooth side, rough side, and edge of the original nickel mesh. After copper deposition, the mesh had 3 μm hole widths as shown in the lower right SEM image. There is significant damping of the transmission with the successive coatings, and molecular absorptions are evident (indicated with the long solid ovals).

infrared (FTIR) spectrometers[20−24] in transmission mode, i.e., ones equipped with DTGS crystal detectors rather than liquid nitrogen cooled MCT detectors. The recorded zero-order transmission spectra show transmission resonances with the maxima often exceeding the fractional open area of the perforated metal film; in other words, they exhibit Ebbesen's extraordinary transmission effect.[21,25,26] This effect is thought to be facilitated by surface plasmons (SPs) in which light coupling to the periodic curvatures of the metal surface excites coherent oscillations in the metal's conducting electrons at the surface.[21,25,26] SPs propagate along the surface at almost the speed of light until they come to a neighboring hole, where they can be transformed back into IR photons without being knocked out of the incident beam. The micrometer-scale distances traversed along the surface between holes (perpendicular to the incident beam) offer a substantial path length for absorption by surface molecules, and we have observed 100- to 1000-fold enhancements in absorption over literature reports.[20−24]

Enhanced IR absorption spectra vs temperature were recorded on the anhydrous trilayer system in order to characterize the states of the phospholipid involved in the phase transition. Polarized optical microscope images vs temperature were used to demonstrate optothermal switching. The difference in optical activity of the lamellar gel and liquid crystalline phases of the DPPC layer[27−30] (with the polarizers set at a critical angle) is enough to control the passage of polarized light through an array of microchannels ∼3 μm wide.

Experimental Section

The finest, commercially available, free-standing, biperiodic, metallic mesh known to us comes from Precision Eforming of Cortland, NY. The nickel mesh has an array of uniform square holes of ∼6.5 μm width on the shiny side tapering to ∼5.5 μm width on the dull side, with a hole-to-hole spacing of 12.7 μm and a thickness of about 1.5−3 μm. Scanning electron microscope (SEM) images of the front, back, and thickness of the starting mesh are given in Figure 3 as insets. A method to uniformly coat the nickel mesh with copper by electrodeposition[20−24] has been developed using copper sulfate solution. A scanning electron microscope image of the mesh after electrochemical coating with copper is given in Figure 3 as an inset at the middle right. For this experiment, the copper coating served two purposes: (1) the hole size of the mesh can be uniformly reduced to the optimal 3−5 μm size range which narrows the resonances while maintaining acceptable transmissions, and (2) alkanethiol monolayers are more stable on copper oxide than on nickel oxide.[31]

Many recipes exist for forming alkanethiol self-assembled monolayers (SAMs).[13−15,32−34] These monolayers were formed by immersing the mesh overnight in a covered beaker of 20 mM solution of 1-hexadecanethiol [$CH_3(CH_2)_{15}SH$] in toluene at room temperature. This solute attaches to the surface by the S−H thiol group, giving up a hydrogen atom and leaving the 16-carbon-long hydrocarbon chain attached to the surface through the sulfur atom. Immersion overnight is much longer than the minimum requirement, but improves the quality of the monolayer. Covering the beaker prevents evaporation of the toluene and the formation of multilayers. The meshes were removed from the solution and allowed to dry overnight at room temperature. Narrowing of the C−H stretch IR absorption features over the course of a day in other experiments has been observed, which is likely associated with ordering of the monolayer on a much slower time scale than the assembly of the monolayer.

There are many strategies for depositing phospholipid bilayers.[10,35−37] In this work phospholipid bilayers were added by dipping the alkanethiol monolayer mesh in a 5 mM solution of L-DPPC in dichloromethane (as supplied) at room temperature five times for 5 s with a 10 s drying time between dips.[38] By withdrawing the meshes from solution into air, the outer layer is expected to consist of hydrophobic chains facing outward. The multiple dipping with this recipe helps to make a better quality DPPC bilayer rather than building up multilayers as can be monitored by the IR absorption spectra. The trilayer mesh system was allowed to dry (and perhaps self-order) overnight at room temperature.

Zero-order IR transmission spectra of the bare copper-coated mesh (top dashed trace), the hexadecanethiolate monolayer

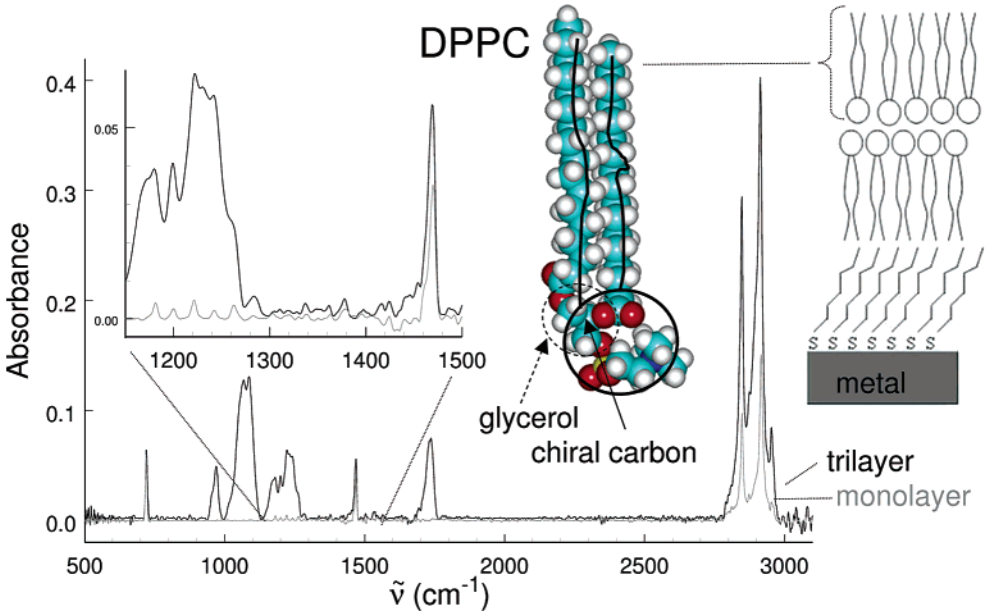

Figure 4. Absorption spectra of the 1-hexadecanethiol monolayer (bottom gray trace) and DPPC/hexadecanethiol trilayer (top black trace) on copper-coated nickel. The region of the CH_2 wagging progression has been expanded in the inset. The intensity of the DPPC/hexadecanethiol assembly relative to the hexadecanethiol monolayer suggests that the assembly is a trilayer.

coating (gray trace in middle), and the DPPC bilayer/hexadecanethiolate trilayer coating (bottom solid trace) are shown in Figure 3. They were obtained on a Perkin-Elmer Spectra GX FTIR (each trace is 300 scans, at 4 cm^{-1} resolution, with a DTGS detector, requiring ~30 min). The transmission spectra are dominated by transmission resonances, of which the most prominent have been labeled as (1,0) and (1,1) in Figure 3. These designations refer to steps along the square reciprocal lattice and also label diffraction spots. The resonances correspond to wavenumbers at which these diffraction spots are no longer transmitted and are instead caught as evanescent waves on the surface of the metal mesh. Also apparent in these transmission curves are dips that correspond to molecular absorptions, of which a few regions (CH stretch, C═O stretch, and CH_2 bend) have been indicated with ovals. While it is very impressive that molecular absorptions can be observed for one-molecule-thick coatings, the resonances provide a less than ideal background. Smooth backgrounds were obtained by applying a spline fit to points chosen along the transmission trace excluding the absorption features. Absorption spectra shown herein correspond to the negative logarithm of the transmission trace divided by its smooth spline background, as shown in Figure 4. The integrated intensity of the CH_2 stretch and bend regions is ~3 times the value for the monolayer, suggesting that on average a trilayer has been assembled, but this conclusion is fraught with assumptions which are discussed in the section IR Absorption Spectra of Supported DPPC Nanocoatings.

The top phospholipid layer could be removed from the trilayer assembly by dipping in water to obtain a bilayer assembly (see far right drawing of Figure 2 vs the middle drawing). In the course of pursuing these experiments, it was discovered that the phospholipid coatings help protect the underlying alkanethiol monolayer from chemical attack by oxygen. That is, these experiments can be accomplished on bare nickel mesh with two main exceptions: (1) these mesh were not allowed to dry overnight before dipping in DPPC since alkanethiol monolayers are not as stable on nickel oxide as copper oxide,[31] and (2) the top layer was removed by placing the mesh in a beaker of distilled water after creation of the DPPC bilayer, agitating the beaker for about 30 s, and blotting the mesh on filter paper upon

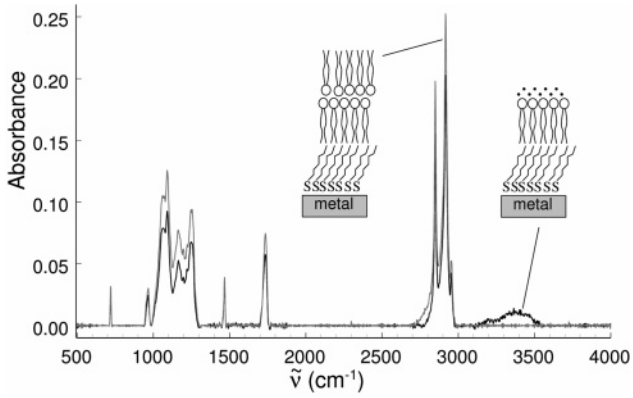

Figure 5. Spectra recorded before and after the removal of the top DPPC layer (on nickel). Note the decrease in the intensity of the CH stretch (~2900 cm^{-1}) and the two water absorptions at ~3200 and 3400 cm^{-1} after the water treatment.

removal.[10] To ensure that only a monolayer of DPPC remained, water drop tests and spectra were completed before and after removal of the top layer. Water drop tests showed that initially the system was hydrophobic: the water drop beaded up on the mesh surface. After the treatment with distilled water, the water drop immediately flattened on the surface of the mesh, as expected for a hydrophilic surface. IR absorption spectra were recorded of the trilayer assembly on nickel before and after treatment in water, as shown in Figure 5. In comparing the before and after spectra, two major differences were noted. The integrated peak area of the CH stretch region showed ~30% decrease in absorption (about the expectation for loss of the top layer in the trilayer), and the final spectrum has peaks for two types of water molecules, located at ~3200 and ~3400 cm^{-1}, illustrating two types of strongly bound water in the system. Both sets of results support the conclusion that the top DPPC layer was removed.

Thermal optical properties were studied using a home-built temperature-controlled cell[39,40] that was machined from an alumina block (~11 cm × 10 cm × 3 cm) with a central window allowing a beam of light to pass. The unit was small enough to fit into an FTIR spectrometer. Spectra of the

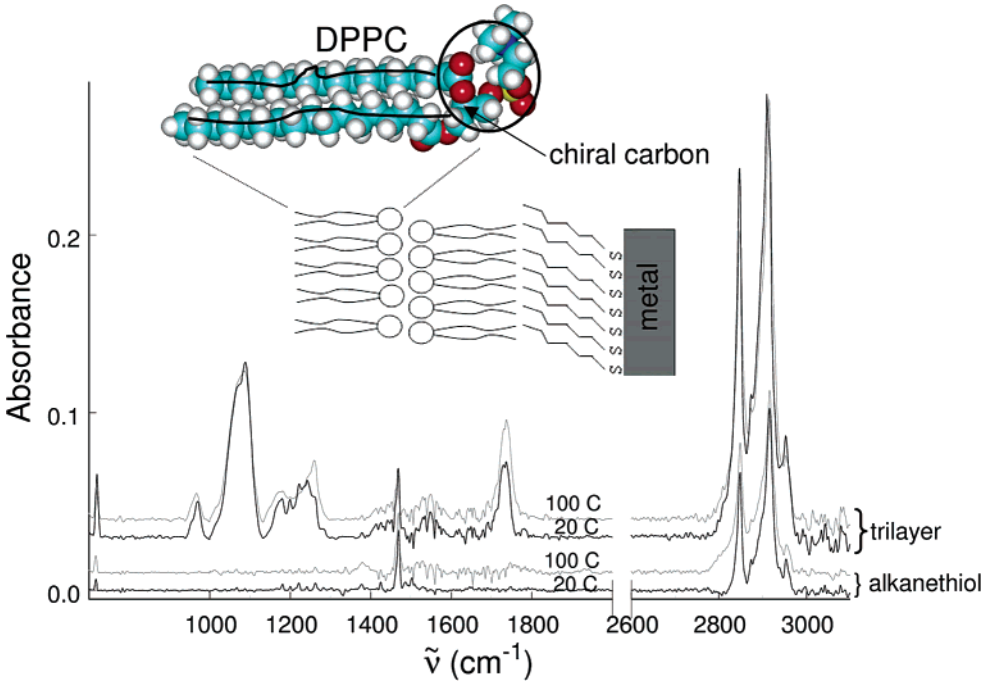

Figure 6. Absorption spectra (with offsets) of 1-hexadecanethiol at 20 and 100 °C and the trilayer assembly at 20 and 100 °C. While no change in the alkanethiol absorbances was noted for this temperature change, the L-DPPC/hexadecanethiol assembly showed a general decrease in intensity of the peaks and a shift in their peak centers which is indicative of phase.

nonhydrated trilayer and bilayer assemblies were recorded as a function of temperature, as shown in Figure 6. The unit was also thin enough (~1 cm at the window) to fit between a microscope stage and a medium-magnification objective. Temperature was controlled by two Peltier elements. Water flowing through a channel in the base kept it at a constant temperature to serve as a reference point for one side of the Peltier elements. A Labview[41] program, written in-house, regulated the voltage applied to the Peltier elements using PID control and temperature feedback from a thermistor positioned near the sample, giving an overall accuracy of ±2 °C in the temperature readings. The eyepiece holder and eyepieces of an ordinary optical microscope (ABCO Model No. 002450) were removed and replaced by an Intel Play QX3+ microscope color camera system (VV6404 CIF CMOS detector chip from VLSI Vision) set on 60×, allowing color images to be captured on a PC through a USB port. Pieces of 1-mm-thick, linearly polarized film were placed between the microscope lamp and sample and between the sample and camera, which could be rotated relative to each other to set the polarization angle difference. A DPPC/hexadecanethiol coated mesh and a drop of water were sandwiched between a glass microscope slide and coverslip to hydrate the system for imaging with the optical microscope. Similar experiments were performed on both a blank mesh and a piece of mesh coated with alkanethiol. No appreciable change in polarized light transmission occurred as the temperature increased in either of these controls. Optically active phospholipid was essential for the thermooptical effect.

Results and Discussion

Thermooptical Switching. Optical images of the fully hydrated trilayer assembly (initial L-DPPC inverted bilayer) were recorded in transmission mode every 3 °C from 20 to 50 °C using the 40× objective lens of the light microscope and polarizers offset by 45° (see Figure 7). These images are cropped (~20% shown) from the full images. Each light spot in the image corresponds to an individual hole in the mesh with a square-lattice hole-to-hole spacing of 12.7 μm. The light spots disappeared between 38 and 41 °C and returned when the system was cooled back to 20 °C. Interestingly, the mesh itself is optically active as a result of spiraling edges at the interfaces of nanocrystallite.[42−44] The activity varies slightly from place to place on the mesh and with different batches of mesh, so the optimal setting of the polarizers might vary somewhat with different experiments. IR absorption experiments performed after the optical microscopy showed the loss of ~30% of the CH stretching intensity, suggesting that the top DPPC layer was lost on average in these experiments as a result of exposure to water. This implied that the optothermal behavior might have been due to a single remaining monolayer of L-DPPC; however, there were other possibilities associated with the lost top layer. Consequently, these experiments were repeated with only a monolayer of L-DPPC at the outset (assemblies as shown on the right side of Figure 5 or 2). For this experiment, images were recorded every 5 °C from 20 to 50 °C, and similar results were obtained (see Figure 8). In addition, IR absorption spectra recorded after removal of the top lipid layer and following the optothermal experiment show similar IR absorptions, demonstrating that the nominal monolayer of phospholipid was not lost during the imaging process. Figures 7 and 8 present the central result of this paper, namely that the phase state of a monolayer of optically active phospholipid (L-DPPC) can control whether light flows through microchannels when a set of polarizers selects light that has been rotated by the metal surface. This transition of a hydrated monolayer of L-DPPC is consistent with the 35−40 °C transition of fully hydrated bilayers of DPPC in bulk systems.

Contribution of Phospholipid Bilayers to the Extraordinary Transmission Effect. The extraordinary IR transmission of the metal mesh enables detailed examination of coatings of a few nanometers in width, so it is notable that increased temperature can also enhance the IR transmission. The room-temperature, zero-order, IR transmission spectra of Cu-coated mesh with ~3 μm hole width in Figure 3 show that, in general,

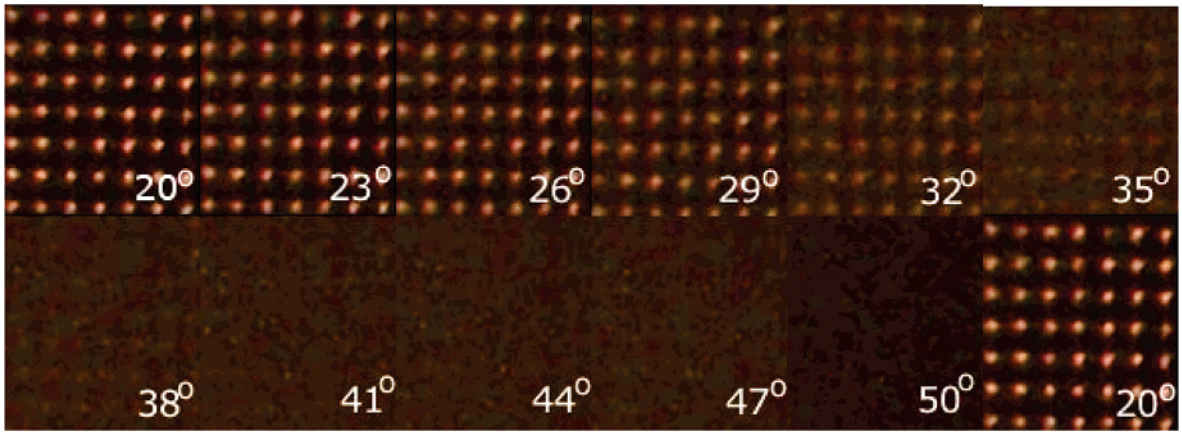

Figure 7. Polarized optical microscope images, with polarizers set at 45°, of copper-coated mesh covered with an initial hydrated trilayer system (hexadecanethiol monolayer/L-DPPC inverted bilayer) vs temperature (°C). The top layer is removed under these circumstances. Images were recorded every 3 °C with about a 2 min equilibration time at each temperature. As the temperature increases, the phase of L-DPPC changes, which modifies the rotation of the polarized light, preventing the passage of light through the mesh. Upon cooling (~30 min after reducing the temperature), transmission returns.

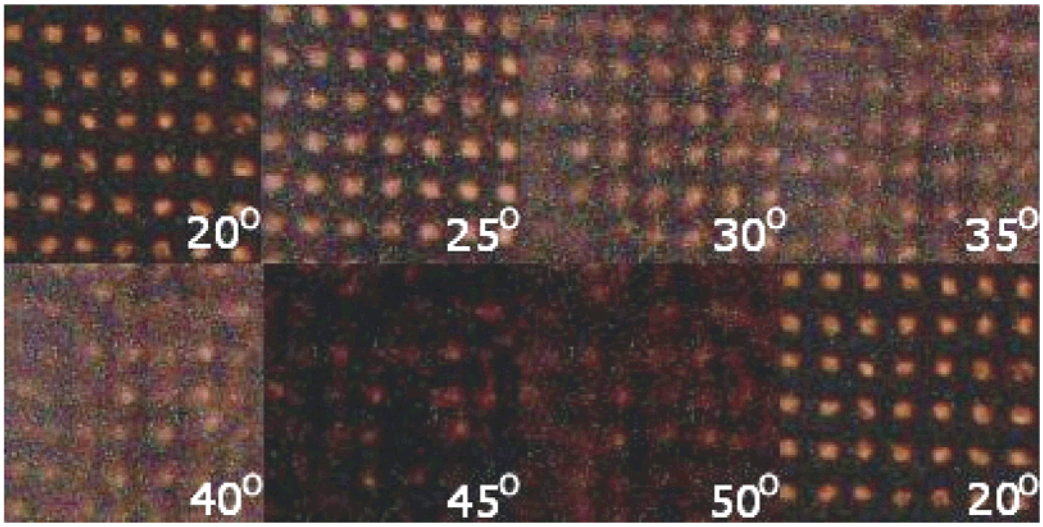

Figure 8. Polarized optical microscope images, with polarizers set at 45°, of mesh coated with a bilayer system (L-DPPC top monolayer/hexadecanethiol monolayer) vs temperature (°C). Images were recorded every 5 °C with about a 2 min equilibration time at each temperature. Upon cooling (~30 min after reducing the temperature), transmission returns.

successive coatings decrease or damp the transmission and shift the surface plasmon resonances, labeled (1,0) and (1,1), to lower frequency. While control experiments showed no change in the transmission of the bare copper mesh from 20 to 100 °C, increased temperature of the molecular coatings increased transmission as shown in Figure 9, where the solid traces are at 20 °C and the dotted traces are at 100 °C. The hexadecanethiolate monolayer showed a small increase of ~2% over the 20−100 °C temperature range on the primary (1,0) transmission resonance, while the trilayer system showed a much larger increase of 20%. Considering that the fractional open area of the copper mesh is ~6%, the warmer phospholipid bilayer enables an additional amount of light to pass that is equivalent to almost half of that incident on each hole. Since the phospholipid bilayer is optically active and changes phase over this temperature range, while the alkanethiolate monolayer is not optically active nor changing in phase, it is evident that the phase of the bilayer is very important in the transmission process. Even in transmission, molecular absorptions are visible (as circled in Figure 3), such as the CH stretches at ~2900 cm^{-1}, the C═O stretch at ~1730 cm^{-1}, and the CH_2 bend at ~1465 cm^{-1}. In the following paragraphs, we undertake a closer examination of the temperature dependence of the IR absorption spectra to better establish the phases involved.

IR Absorption Spectra of Supported DPPC Nanocoatings. The absorption spectra of the alkanethiol SAM and the trilayer system at room temperature are shown in Figure 4. Lists of the vibrations and their intensities in each spectrum are given in Table 1 for the hexadecanethiol SAM and Table 2 for the L-DPPC bilayer/hexadecanethiol SAM trilayer in which assignments have been confirmed by previous work.[11,13,45−48] The absorption in this work of the CH_2 asymmetric stretch for hexadecanethiol on copper (0.15 at 2916.6 cm^{-1}) is >300 times the bilayer absorption seen with reflection absorption infrared spectroscopy (RAIRS) (absorbance of 0.000 48[13]). If there were resonant enhancements, absorptions would be more intense when a vibration lies at a transmission resonance maximum. For most of the spectral range, no significant changes in the absorption spectra have been found[23] upon dispersing the resonances by angling the mesh, although we are still working on this issue for vibrations near the primary transmission resonance at ~720 cm^{-1}. Consequently, it is currently believed that the enhancement is generally dominated by a path-length effect associated with the distance that the surface plasmons (SPs)

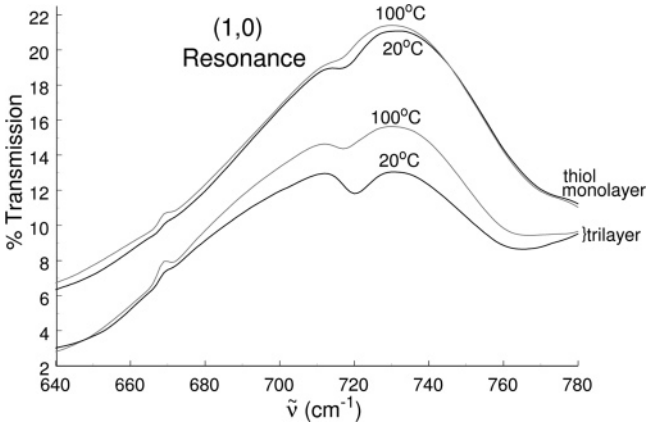

Figure 9. Transmission spectra of (1,0) resonance with 1-hexadecanethiol at 20 and 100 °C (top traces) and 1-hexadecanethiol/L-DPPC inverted bilayer assembly at 20 and 100 °C (bottom traces) with different meshes than earlier figures and no hydration. There were no changes evident with the bare mesh, and only a slight increase (about 2%) in the transmission of the primary resonance was noted with the thiol monolayer. However, a 20% increase (15.7% at 100 °C versus about 13% at 20 °C) was noted for the same temperature change with the trilayer assembly.

TABLE 1: IR Absorption Vibrational Frequencies and Relative Intensities of 1-Hexadecanethiol Monolayer at Room Temperature[a]

freq (cm^{-1})	assignment	rel int
2953.5	CH_3 asym stretch	0.112
2916.6	CH_2 asym stretch	1.000
2873.3	CH_3 sym stretch	0.141
2848.4	CH_2 sym stretch	0.648
1470.0	CH_2 asym bend	0.232
1379.1	CH_3 umbrella	0.017
1320.8	W_8	0.007
1303.1	W_7	0.010
1283.0	W_6	0.005
1262.7	W_5	0.025
1242.5	W_4	0.015
1221.5	W_3	0.032
1200.2	W_2	0.018
1181.4	W_1	0.028
719.6	CH_2 rock	0.404

[a] The intensities are just the absorbances at peak maximum relative to an absorbance value of 0.151 for the asymmetric CH_2 stretch; i.e. they have not been deconvolved from overlapping features.

travel between holes along the surface. The path length for absorption in the Laibinis et al. RAIRS experiment[13] can be estimated as 50 nm (using an 85° incident angle, an 18° hexadecanethiolate tilt angle, and a 2.2 nm layer thickness), so the ratio of the absorbances in our experiment and the RAIRS experiment implies a path length of ~16 μm (shared on both sides of the mesh). Similarly, the C═O absorption of 0.000 55 at 1737 cm^{-1} seen by Meuse et al.[10] for a supported DPPC bilayer corresponds to a path length of 32 nm (using an 75° incident angle, a 0° tilt angle, and a 4.1 nm estimated thickness). The ratio of absorbances in our experiment and the Muese experiment implies a path length of ~4 μm. Basically, the path lengths appear to be on the order of the nearest hole-to-hole spacing, roughly implying that the surface plasmons only travel to the adjacent hole before coupling out as photons. This suggests that a Beer's law approach to the data may be useful.

The hexadecanethiolate IR absorption spectrum is shown as the bottom gray trace in Figure 4. This spectrum has been previously studied by us.[24] The Snyder CH_2 wagging progression transitions[47,49] are observed (see the expanded inset of Figure 4 in the range from 1180 to 1330 cm^{-1}), suggesting that

TABLE 2: IR Absorption Vibrational Frequencies and Relative Intensities of 1-Hexadecanethiol SAM/L-DPPC Bilayer Assembly at Room Temperature[a]

freq (cm^{-1})	assignment	rel int	temp shift from 20 to 100 °C (cm^{-1})
2953.7	CH_3 asym stretch	0.206	0.0
2914.0	CH_2 asym stretch	1.000	1.5
2875.0	CH_3 sym stretch	0.287	0.0
2847.7	CH_2 sym stretch	0.731	0.9
1737.6	C═O stretch	0.182	1.9
1469.5	CH_2 asym bend	0.136	−0.6
1377.9	CH_3 umbrella	0.008	
NA	W_8		
NA	W_7		
1286	W_6		
1263	W_5		
1243	W_4		
1241.8	PO_2^- asym stretch	0.141	17.4
1222	W_3		
1199.9	W_2		
1181	W_1		
1180.2	C−C stretch	0.093	1.5
1087.6	PO_2^- sym stretch	0.321	−2.1
970.2	CNC sym stretch	0.118	−3.0
720.5	CH_2 rock	0.156	−1.3

[a] The intensities are given as peak heights relative to an absorbance of 0.41 for the asymmetric CH_2 stretch. Temperature shifts are given in the last column for a change from 20 to 100 °C.

the sample is dominated by the all-trans configuration of the hydrocarbon chains which is characteristic of more crystalline phases. The observed symmetric (2848.4 cm^{-1}) and asymmetric (2916.6 cm^{-1}) CH_2 stretches lie to the unmelted side of the range associated with chain melting.[50] This and the lack of splitting of the asymmetric bending peak (~1470 cm^{-1}) indicate the crystalline gel phase (as expected from bulk). Control experiments[51] at many temperatures (see Figure 6) reveal no significant changes over the range from 20 to 100 °C; i.e., the underlying monolayer remains in the gel crystalline phase over the course of these experiments because the gel crystalline to liquid crystalline transition is at a temperature >100 °C.

The spectra of the trilayer (see Figures 6 and 9) exhibit important contributions from the L-DPPC bilayer. Note the C═O stretches (at 1737.6 cm^{-1}) which give a unique DPPC signature in a region undisturbed by the underlying monolayer. The DPPC vibrations also convey information about the phase of the bilayer part of this system.[50] The observed CH_2 asymmetric stretch (2914.0 cm^{-1}) and CH_2 symmetric stretch (2847.7 cm^{-1}) with no hydration both lie to the red side of the chain melting transition, indicating that the phospholipid bilayer chains are not melted at the lower temperatures. Temperature studies show a blue shifting of 1.5 and 0.9 cm^{-1} from 20 to 100 °C for these vibrations, respectively, revealing chain melting. The CH_2 rocking transition (720.5 cm^{-1}) and the CH_2 asymmetric bending transition (1469.5 cm^{-1}) shift in the opposite direction with chain melting (see Table 2), just as in the bulk system. Upon chain melting,[51] these vibrations tend to have their widths increase and their integrated intensities decrease, which is attributed to "increased chain mobility and gauche rotomer content".[50] The upper traces of the inset in Figure 4 show that the Snyder wagging progression is also observed with the DPPC bilayer. This progression of peaks lies on top of broader transitions such as the PO_2^- asymmetric stretch and C−C stretch. Deconvolution (with $\Gamma = 1$ and no smoothing) enabled the peaks to be better located, giving the values reported in Table 2. The appearance of the Snyder wagging progression means there exist all-trans hydrocarbon chains in the DPPC at lower temperatures. The wagging progressions vanish upon chain melting,[50] leaving a

residual that we presume is associated with the unmelted underlying monolayer. The lack of fine structure (C═O stretch at 1737.6 cm $^{-1}$, CH_2 rocking transition at 720.5 cm^{-1}, CH_2 asymmetric bending transition at 1469.5 cm^{-1})[50]at the lowest temperatures suggests a lamellar gel phase of the DPPC rather than a fully crystalline phase. The behavior of the peak profiles, peak shifts, and peak intensity changes with temperature are all consistent with well-characterized phase changes in phospholipid bilayers.[50,52] Namely, the DPPC bilayer in our trilayer system starts in the lamellar gel phase and with heating transforms into a more fluid, liquid crystalline phase. The underlying alkanethiol monolayer remains in a chain-ordered phase in the temperature range studied.

Quantifying the Layering. One expects the minimal assembly to be an inverted bilayer of phospholipid upon the alkanethiolate monolayer, but one might just as reasonably have any multiple of phospholipid bilayers upon the alkanethiolate monolayer. Noting that the phospholipid and the alkanethiol have the same hydrocarbon chain lengths (16 carbons), we use the absorbance of common methylene sequences of vibrations of the alkanethiol self-assembled monolayer as a rough calibration for the thickness of the phospholipid layer. The integrated intensity of the CH stretch region is 3.7 times the value for the hexadecanethiol monolayer, and 3.3 times the monolayer value in the CH_2 bend region at 1470 cm^{-1}. The CH_2 rock region at 720 cm^{-1} (showing a ration of 1.3) was not used because our many observations of the CH_2 rock in alkanethiol SAM spectra[24] show that the intensity of this mode varies relative to the rest of the spectrum—perhaps being particularly sensitive to the phase and ordering of the monolayer or due to coupling with the primary surface plasmon resonance [(1,0) at ~720 cm^{-1}]. There are a number of factors that complicate the quantitative comparison in this manner, such as surface selection rules with regard to molecular orientation, the phase and ordering of the layers, adsorbate/surface-plasmon coupling, and adsorbate coupling to the metal surface. Assuming negligible differences in the CH_2 chain angles relative to surface normal, ~10-μm-scale attenuation of the IR plasmon radiation field intensity from the metal surface which is large compared to the molecular layer thickness, and no significant electronic enhancement differences of the hydrocarbon by the metal surface, these results support the formation of a trilayer on average, just as expected from the dipping recipe.

Shifts of the (1,0) transmission resonance upon coating are evident in Figure 3 that are diagnostic for the dielectric and thickness of the coatings. These shifts are wavelength-scanned analogues[53] to the attenuated total reflection[54,55] (ATR) resonances which are well-known to be very sensitive to nanocoatings. The (1,0) resonance of the uncoated mesh occurs at 760 cm^{-1}, which is shifted from its expected position (787 cm^{-1} based on the lattice spacing of the grid) due to oxides and the thinness splitting.[56] This peak shifts to 755 cm^{-1} upon coating with the hexadecanethiol monolayer, and then to 723 cm^{-1} with the DPPC bilayer (as determined by removing the absorption feature with a simulated Gaussian line shape). Thus, a shift of 5 cm^{-1} is observed with the alkanethiol SAM and 37 cm^{-1} with the trilayer from the uncoated mesh. If we take 5 cm^{-1} as characteristic of the shift from a 2-nm-thick coating with a dielectric constant of 2.1, then a DPPC bilayer of 5 nm thickness[57,58] and an effective dielectric constant of 5 would be expected to produce a (5/2.1)(5/2)5 cm^{-1} = 30 cm^{-1} shift. By this simple picture, the trilayer is predicted to have a shift of 5 + 30 = 35 cm^{-1}, which is close to that observed. Certainly, much more carefully controlled experiments on the transmission resonant shifts are desirable; however, the combination of dielectric and/or thickness determinations with IR absorption spectra shows great potential for better characterization of surface coatings.

Conclusion

The phase transitions of bulk phospholipids are well-known to involve sufficient changes in optical rotation that such studies are routinely accomplished by polarized light microscopy,[19,59] so it is the effect of the microchannels that is interesting in this work. The active element in Figures 7 and 8 was an L-DPPC monolayer which diminished visible transmission in the vicinity of the bulk chain melting transition temperature.[10] The change is reversible. As the system cools, the light "switches" on again, acting like a thermooptical switch. While efforts were concentrated on the thermooptical switching, it may well turn out that the ability to assay nanocoatings in constricted spaces with enhanced IR absorption spectroscopy and transmission resonance shifts are more important contributions. There is a prospect of using these strategies to construct and assay nanoassemblies in an individual microchannel, as we have recently obtained comparable IR absorption spectra on 10-μm-wide spots in an IR microspectrometer, i.e., from the region of a single microchannel. Promising work is also being pursued that involves trapping phospholipid bilayers between a stack of two pieces of metallic microarray.

Acknowledgment. The Coe group thanks the ACS PRF (Grant 42452-AC5) and the NSF (Grant CHE-0413077) for support; the Caffrey group thanks the Science Foundation Ireland (O2-IN1-B266) and the National Institutes of Health (GM61070, GM075915).

References and Notes

(1) Ebbesen, T. W.; Lezec, H. J.; Ghaemi, H. F.; Thio, T.; Wolff, P. A. *Nature (London)* **1998**, *391*, 667.

(2) Kim, T. J.; Thio, T.; Ebbesen, T. W. (Nec Research Institute, Inc., USA). Optical transmission control apparatus utilizing metal films perforated with subwavelength-diameter holes. In U.S. Patent 6,040,936, 2000.

(3) Kim, T. J.; Thio, T.; Ebbesen, T. W.; Grupp, D. E.; Lezec, H. J. *Opt. Lett.* **1999**, *24*, 256.

(4) Dintinger, J.; Klein, S.; Ebbesen, T. W. *Adv. Mater. (Weinheim, Germany)* **2006**, *18*, 1267.

(5) Burger, P. *Angew. Chem., Int. Ed.* **2001**, *40*, 1917.

(6) Yang, J.; Zhou, Q.; Chen, R. T. *Appl. Phys. Lett.* **2002**, *81*, 2947.

(7) Christie, W. W. Phosphatidylcholine and Related Lipids. www.lipid.co.uk; 2003.

(8) Albert, B.; Bray, D.; Lewis, J.; Raff, M.; Roberts, K.; Watson, J. D. *Molecular Biology of the Cell*; Garland Publ. Inc.: New York, 1994.

(9) Hentschel, M.; Hosemann, R.; Helfrich, W. *Z. Naturforsch.* **1980**, *35A*, 643.

(10) Meuse, C. W.; Krueger, S.; Majkrzak, C. F.; Dura, J. A.; Conner, J. T.; Plant, A. L. *Biophys. J.* **1998**, *74*, 1388.

(11) Arrondo, J. L. R.; Goni, F. M. *Chem. Phys. Lipids* **1998**, *96*, 53.

(12) Cevc, G.; Marsh, D. Bilayer Properties. In *Phopholipid Bilayers: Physical Principles and Models*; John Wiley & Sons: New York, 1987.

(13) Laibinis, P.; Whitesides, G. M.; Allara, D. L.; Tao, Y.-T.; Parikh, A. N.; Nuzzo, R. G. *J. Am. Chem. Soc.* **1991**, *113*, 7152.

(14) Jennings, G. K.; Munro, J. C.; Yong, T.-H.; Laibinis, P. E. *Langmuir* **1998**, *14*, 6130.

(15) Ron, H.; Cohen, H.; Matlis, S.; Rappaport, M.; Rubinstein, I. *J. Phys. Chem. B* **1998**, *102*, 9861.

(16) Yi, P. N.; MacDonald, R. C. *Chem. Phys. Lipids* **1973**, *11*, 114.

(17) Erdei, L.; Csorba, I.; Thuyen, H. X. *Lipids* **1975**, *10*, 115.

(18) Powers, L.; Pershan, P. S. *Biophys. J.* **1977**, *20*, 137.

(19) Petrov, A. G.; Gawrisch, K.; Brezensinski, G.; Klose, G.; Mops, A. *Biochim. Biophys. Acta* **1982**, *690*, 1.

(20) Williams, S. M.; Rodriguez, K. R.; Teeters-Kennedy, S.; Shah, S.; Rogers, T. M.; Stafford, A. D.; Coe, J. V. *Nanotechnology* **2004**, *15*, S495.

(21) Williams, S. M.; Stafford, A. D.; Rodriguez, K. R.; Rogers, T. M.; Coe, J. V. *J. Phys. Chem. B* **2003**, *107*, 11871.

(22) Williams, S. M.; Stafford, A. D.; Rogers, T. M.; Bishop, S. R.; Coe, J. V. *Appl. Phys. Lett.* **2004**, *85*, 1472.
(23) Williams, S. M.; Rodriguez, K. R.; Teeters-Kennedy, S.; Stafford, A. D.; Bishop, S. R.; Lincoln, U. K.; Coe, J. V. *J. Phys. Chem. B* **2004**, *108*, 11833.
(24) Rodriguez, K. R.; Shah, S.; Williams, S. M.; Teeters-Kennedy, S.; Coe, J. V. *J. Chem. Phys. B* **2004**, *121*, 8671.
(25) Martin-Moreno, L.; Garcia-Vidal, F. J.; Lezec, H. J.; Pellerin, K. M.; Thio, T.; Pendry, J. B.; Ebbesen, T. W. *Phys. Rev. Lett.* **2001**, *86*, 1114.
(26) Ebbesen, T. W.; Lezec, H. J.; Ghaemi, H. F.; Thio, T.; Wolff, P. A. *Nature* **1998**, *391*, 667.
(27) Lis, L. J.; McAlister, M.; Fuller, N.; Rand, R. P.; Parsegian, V. A. *Biophys. J.* **1982**, *37*, 657.
(28) Lis, L. J.; McAlister, M.; Fuller, N.; Rand, R. P.; Parsegian, V. A. *Biophys. J.* **1982**, *37*, 667.
(29) Rand, R. P.; Das, S.; Parsegian, V. A. *Chem. Scr.* **1985**, *25*, 15.
(30) Rand, R. P.; Parsegian, V. A. *Biochim. Biophys. Acta* **1989**, *988*, 351.
(31) Mekhalif, Z.; Riga, J.; Pireaux, J.-J.; Delhalle, J. *Langmuir* **1997**, *13*, 2285.
(32) Fritz, M. C.; Carraro, C.; Maboudian, R. *Tribol. Lett.* **2001**, *11*, 171.
(33) Sung, M. M.; Sung, K.; Kim, C. G.; Lee, S. S.; Kim, Y. *J. Phys. Chem. B* **2000**, *104*, 2273.
(34) Vollmer, S.; Fouquet, P.; Witte, G.; Boas, C.; Kunat, M.; Burghaus, U.; Woll, C. *Surf. Sci.* **2000**, *462*, 135.
(35) Plant, A. L. *Langmuir* **1993**, *9*, 2764.
(36) Plant, A. L.; Gueguetchkeri, M.; Yap, W. *Biophys. J.* **1994**, *67*, 1126.
(37) Tien, H. T.; Salamon, Z. *Biotechnol. Appl. Biochem.* **1990**, *12*, 478.
(38) Hianik, T.; Fajkus, M.; Sivak, B.; Rosenberg; Kois, P.; Wang, J. *Electroanalysis* **2000**, *12*, 495.
(39) Caffrey, M. Personal communication, 2003.
(40) Misquitta, L. V.; Misquitta, Y.; Mohan, J. M.; Hart, D.; Zhalnina, M.; Cramer, W. A.; Caffrey, M. *Structure* **2004**, *12*, 2113.
(41) *LabView 5.0 Graphical Programming for Instrumentation*; National Instruments Corporation: Austin, TX, 1998.
(42) Hovarth, J. D.; Gellman, A. J. *Top. Catal.* **2003**, *25*, 9.
(43) Lepeshkin, N. N. Optical Properties of Metal-Dielectric Composites. Ph.D. Thesis, New Mexico State University, 2001.
(44) Schaaff, T. G.; Whetten, R. L. *J. Phys. Chem. B* **2000**, *104*, 2630.
(45) Akutsu, H. *Biochemistry (Moscow)* **1981**, *20*, 7359.
(46) Hou, Z.; Abbott, N. L.; Stroeve, P. *Langmuir* **1998**, *14*, 3287.
(47) MacPhail, R. A.; Strauss, H. L.; Snyder, R. G.; Elliger, C. A. *J. Phys. Chem.* **1984**, *88*, 334.
(48) Twardowski, J.; Anzenbacher, P. *Raman and IR Spectroscopy in Biology and Biochemistry*; Ellis Horwood: New York, 1994.
(49) Snyder, R. *J. Mol. Spectrosc.* **1960**, *4*, 411.
(50) Lewis, R. N. A. H.; McElhaney, R. N. Fourier Transform Infrared Spectrscopy in the Study of Hydrated Lipids and Lipid Bilayer Membranes. In *Infrared Spectroscopy of Biomolecules*; Mantsch, H. H., Chapman, D., Eds.; Wiley-Liss, Inc.: New York, 1996; p 159.
(51) Teeters-Kennedy, S. The Extraordinary Transmission of Subwavelength Metallic Arrays: An Infrared Study of the Self-Assembly of Phospholipid Bilayers on Alkanethiol Monolayers. Master's Thesis, The Ohio State University, 2004.
(52) Casal, H. L.; Mantsch, H. H. *Biochim. Biophys. Acta* **1983**, *735*, 387.
(53) Lirtsman, V.; Ziblat, R.; Golosovsky, M.; Davidov, D.; Pogreb, R.; Sacks-Granek, V.; Rishpon, J. *J. Appl. Phys.* **2005**, *98*, 093506.
(54) Malinsky, M. D.; Kelly, K. L.; Schatz, G. C.; Duyne, R. P. V. *J. Am. Chem. Soc.* **2001**, *123*, 1471.
(55) Raether, H. *Surface plasmons on smooth and rough surfaces and on gratings*; Springer-Verlag: Berlin; New York, 1988.
(56) Williams, S. M.; Coe, J. V. *Plasmonics* **2006**, *1*, 87.
(57) Kumar, S.; Hoh, J. H. *Langmuir* **2000**, *16*, 9936.
(58) Nagle, J. F.; Tristram-Nagle, S. *Biochim. Biophys. Acta: Rev. Biomembr.* **2000**, *1469*, 159.
(59) Janiak, M. J.; Small, D. M.; Shipley, G. G. *J. Lipid Res.* **1979**, *20*, 183.